JOURNAL OF GEOPHYSICAL RESEARCH: SPACE PHYSICS, VOL. 118, 533–541, doi:10.1029/2012JA018236, 2013

Lunar and solar tidal variabilities in mesospheric winds and EEJ strength over Tirunelveli (8.7°N, 77.8°E) during the 2009 major stratospheric warming

S. Sathishkumar[1] and S. Sridharan[2]

Received 24 August 2012; revised 15 November 2012; accepted 19 November 2012; published 25 January 2013.

[1] Mesospheric wind observations by the medium frequency radar and geomagnetic field observations at Tirunelveli (8.7°N, 77.8°E, 1.75°N dip angle) are used to study the relative importance of solar and lunar influences in the variabilities of mesospheric tides and equatorial electrojet (EEJ) strength during the unprecedented major stratospheric sudden warming (SSW) of 2009. It is observed that the afternoon reversal in the EEJ, popularly known as counter electrojet, occurs consecutively for several days during the SSW event, when there is an enhancement of solar semidiurnal tide in both zonal wind at 90 km and EEJ strength over Tirunelveli. Although the amplitude of lunar tides also shows enhancement, it is much less than that of solar. The diurnal tidal amplitude in zonal wind and EEJ strength also shows large enhancement just before the onset of SSW. However, solar semidiurnal tide dominates diurnal tide during the SSW. The diurnal tidal phase in zonal wind shifts to a few hours earlier during the SSW. The lunar semidiurnal tidal phase shifts to later hours in both zonal wind and EEJ strength. The main observation of the present study is that the large semidiurnal tide observed during the SSW 2009 is mostly solar driven and only partly lunar driven, although tidal planetary wave interaction also may play a vital role. Although a similar behavior is noticed during the SSW 2006 also, the large lunar semidiurnal tide observed in the EEJ strength without having large lunar semidiurnal tide in the underlying mesospheric winds needs further investigation.

Citation: Sathishkumar, S., and S. Sridharan (2013), Lunar and solar tidal variabilities in mesospheric winds and EEJ strength over Tirunelveli (8.7°N, 77.8°E) during the 2009 major stratospheric warming, *J. Geophys. Res. Space Physics*, *118*, 533–541, doi:10.1029/2012JA018236.

1. Introduction

[2] Atmospheric tides can be both solar and lunar driven. Solar tides are generated due to solar insolation by water vapor in the troposphere, ozone in the stratosphere and N_2 and O_2 in the mesosphere. Lunar tides are generated in the lower atmosphere due to gravitational attraction on the atmosphere and forcing due to vertical movement of ocean and of the Earth's land surface at the lower boundary [*Chapman and Lindzen*, 1970]. The influence of tides on low-latitude ionospheric electrodynamics has been recognized, although the knowledge about the relative importance of solar and lunar tides is lacking, as lunar tides traditionally were considered to be smaller than solar tides. Unlike solar tides, lunar tides show preferential activity during northern hemispheric winter [*Sandford et al*., 2006; *Paulino et al*., 2012]. *Stening et al*. [1996] suggested that the vertical propagation of lunar tides could be favored by the atmospheric conditions associated with the stratospheric sudden warming (SSW), which is an event characterized by a sudden temperature increase in the winter polar stratosphere and deceleration and sometimes reversal in stratospheric zonal winds [*Matsuno*, 1971] due to rapid growth of quasi-stationary planetary waves.

[3] The effect of solar and lunar tides are observed in the equatorial electrojet (EEJ) current [*Stening*, 1991; *Eccles et al*., 2011], which is an intense current system flowing normally eastward during the daytime at an altitude of 105 km in a narrow latitudinal band of ±3° around the dip equator. Sudden changes in the tidal components of the EEJ current, vertical plasma drift and total electron content are suggested to be related to SSW events in the polar atmosphere [*Chau et al*., 2009; *Sridharan et al*., 2009; *Goncharenko et al*., 2010a, 2010b; *Anderson and Araujo-Pradere*, 2010]. The enhancement of semidiurnal tidal amplitude has been suggested to be a reason for the occurrence of counter electrojet (CEJ), which is the reversal of the eastward current system to westward occurring sometimes in the afternoon hours. As the EEJ current system is mainly driven by tidal winds, enhancement semidiurnal tide on some days has been considered as a

[1]Equatorial Geophysical Research Laboratory, Indian Institute of Geomagnetism, Krishnapuram, Tirunelveli, India.
[2]National Atmospheric Research Laboratory, Pakala, India.

Corresponding author: S. Sridharan, National Atmospheric Research Laboratory, Gadanki 517 112, Pakala, India. (susridharan@narl.gov.in)

2169-9380/13/2012JA018236

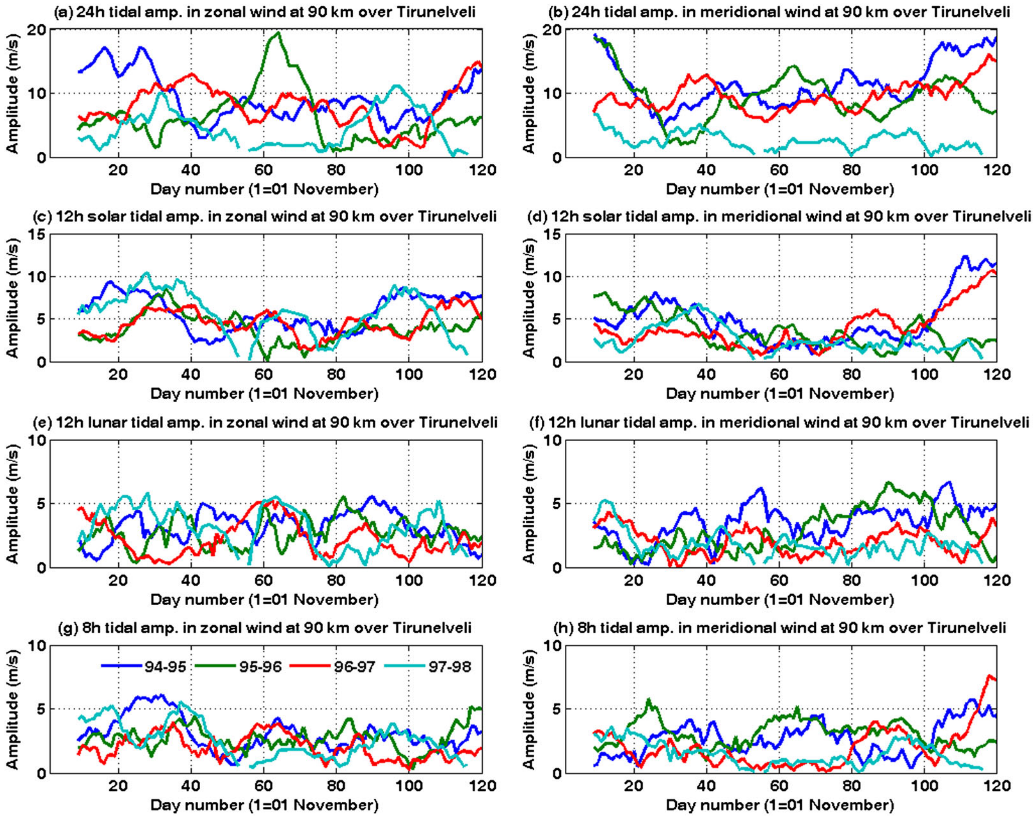

Figure 1. Daily variation of (a,b) diurnal, (c,d) solar semidiurnal, (e,f) lunar semidiurnal, and (g,h) terdiurnal tidal variabilities in zonal and meridional winds at 90 km over Tirunelveli for the winter months (November–February) of nonmajor stratospheric warming years 1994–1995, 1995–1996, 1997–1998 and 1998–1999.

potential reason for the occurrence of CEJ on those days [*Hanuise et al*., 1983, and references therein]. However, it still remains uncertain whether the enhanced semidiurnal tide during SSW events is of solar or lunar origin. Several recent studies have reported that the enhancement of semidiurnal tide during SSWs is solar driven and suggested that these may be related to changes in the ozone [*Sridharan et al*., 2012; *Goncharenko et al*., 2012]. However, *Fejer et al*. [2010] noted a semidiurnal character in vertical plasma drifts at Jicamarca with large downward drifts in the afternoon accompanied by increased upward drifts in the morning close to new or full moon. Besides, the time of maximum downward perturbation becomes later on succeeding days, indicating a possible lunar influence. Similar changes were observed in the ground-based geomagnetic variations ΔH, which occurred earlier and stronger at American longitudes and later and weaker in the Pacific Ocean region [*Stening*, 2011]. However, *Anderson* and *Araujo-Pradere* [2010] examined *F* region drifts, derived from ground-based magnetometers in Peru and in the Philippines during 2003 and 2004 SSWs and found notable correlation with lunar phase. Recently, *Paulino et al*. [2012] showed enhanced lunar semidiurnal tide over the Brazilian sector during the major SSW of 2006. Recently, *Forbes and Zhang* [2012] noted nearly three times enhanced lunar M2 tide of period 12.43 h in Sounding of Atmosphere by Broadband Emission Radiometry temperature measurements at 110 km height over climatogical values during SSW 2009 and attributed it to change in the zonal mean wind distribution in connection with the SSW.

[4] In the present study, both lunar and solar tidal variabilities are presented during the winter of 2008–2009, when major stratospheric warming events occurred. The tidal variabilities are compared with EEJ strength over the Indian sector and discussed.

2. Data Analysis

2.1. Tidal Analysis of MF Radar Winds Over Tirunelveli

[5] The MF radar at Tirunelveli (8.7°N, 77.8°E) operates at 1.98 MHz and it has been providing nearly continuous wind observations in the altitude region 80–98 km with good data acceptance rate. However, the radar winds at higher heights are partly contaminated by the presence of electrojet-driven drift motions. Hence, for the present study, the radar data at 90 km, where the data acceptance rate is larger and influence of drift motions is less, are utilized

[6] Dominant solar tides are diurnal (24 h), semidiurnal (12 h), and terdiurnal (8 h). The migrating lunar semidiurnal tide of period 12.416 to 12.424 h is the largest amplitude mode. Furthermore, the frequencies of the lunar and solar tides are very close. Extended data sets are thus required to

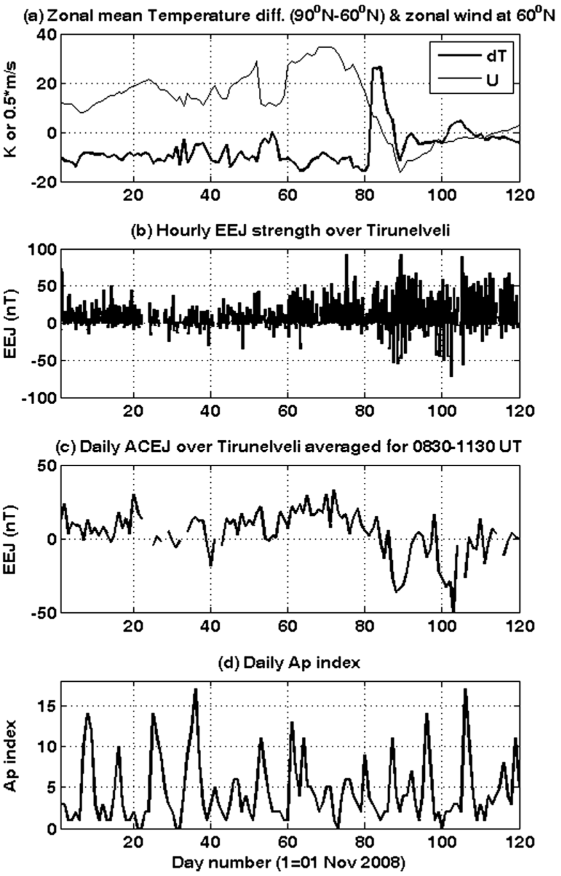

Figure 2. (a) Daily variation of zonal mean temperature difference between the latitudes 90°N and 60°N and zonal mean zonal wind at 60°N; (b) hourly EEJ strength over Tirunelveli; (c) daily afternoon CEJ strength computed by taking average of EEJ strength for 0830–1130 UT (1400–1700 LST, which is five and a half hours ahead of UT); and (d) daily *Ap* index for the time interval of 1–120 d starting from 1 November 2008.

provide the spectral resolution necessary to resolve the lunar and solar components. Hence, a 16 d window of hourly winds at each height is assumed to consist of a mean wind, sinusoidal planetary wave components, solar (diurnal, semidiurnal, and terdiurnal components) and lunar tidal (semidiurnal component) oscillations, as can be seen from the following equation:

$$U = U_o + \sum_{n=1}^{l}\left[A_n\cos\left(\frac{2\pi n}{L}t\right) + B_n\sin\left(\frac{2\pi n}{L}t\right)\right] + \sum_{n=1}^{3}\left[A_n\cos\left(\frac{2\pi n}{24}t\right) + B_n\sin\left(\frac{2\pi n}{24}t\right)\right] + A_L\cos\left(\frac{2\pi}{12}\tau\right) + B_L\sin\left(\frac{2\pi}{12}\tau\right)$$

where U_o is the mean wind, L is the total data length (here 16 d), l is the number of harmonics required to include all planetary wave periods (here $l = 8$ so that waves with periods from 16 to 2 d are included in the fit), t is the solar time and τ is the lunar time. The lunar time given by t-ν, where ν is the lunar age, which is equal to 0 at the new moon and the tidal amplitudes and phases are computed using least squares method [*Stening et al.*, 1994; *Paulino et al.*, 2012]. For checking, we made calculations with different data lengths. However, this method gives unreasonably large amplitudes for lunar tides, when components with periods closer to and greater than 16 d are included in the fit. Hence, the last term of the above equation is replaced by $A_\mathrm{L}\cos\left(\frac{2\pi}{12.42}t\right) + B_\mathrm{L}\sin\left(\frac{2\pi}{12.42}t\right)$, where the lunar time period (12.42 h) is used. As this method of computation gives reasonable amplitudes for lunar tides and the lunar tidal phases computed shows shift toward later hours on successive days, which is a typical behavior of lunar tides, this method is used in the present study. Then the data window is shifted by 24 h successively to compute daily variation of solar and lunar tidal amplitudes and phases. In the present work, the solar and lunar tidal variabilities during the major warming event in 2009 are examined. In order to understand the normal behavior of tidal variabilities over Tirunelveli, tidal variabilities during undisturbed winters are worth to be presented. As no major SSW event occurred during 1993–1998 [*Manney et al.*, 2005; *Sridharan and Sathishkumar*, 2008], the daily tidal variabilities over Tirunelveli at 90 km during these winters are presented in Figure 1. From the figure, it can be observed that the diurnal tidal amplitudes are in general larger than semidiurnal and terdiurnal tidal amplitudes. The solar semidiurnal tidal amplitudes in both zonal and meridional winds are below 10 m/s and lunar semidiurnal tidal amplitudes are below 5 m/s during most of the winter period.

2.2. Geomagnetic Data Over Tirunelveli

[7] The variations in the three components of the geomagnetic field have been recorded by a network of magnetic observatories of the Indian Institute of Geomagnetism located from the magnetic equator to the northernmost Indian latitudes. The EEJ strength is derived from the differences between the magnetic field variations in the horizontal field obtained from Tirunelveli (TIR) (8.7°N, 77.8°E, geographic, 1.75°N dip angle) and Alibag (18.6°N, 72.9°E, geographic, 24°N, dip angle). Tirunelveli is located close to the center of the EEJ and is also under the influence of the *Sq* current system, whereas Alibag is a station under the influence of *Sq* current system only [*Kane*, 1973]. To extract tidal components in EEJ strength, the same method described in the last section is used.

2.3. ERA-Interim Data

[8] To present the state of winter stratosphere during the winters of 2008–2009 and 2005–2006 of major warming events, ERA-interim temperature and winds are used. The interim data are obtained by the European Center for Medium Range Weather Forecasting through their variational data assimilation scheme and are available at six hourly intervals for 37 pressure levels from 1000 hPa to 1 hPa, and for the latitude-longitude grid of 1.5° × 1.5° [*Berrisford et al.*, 2009].

3. Results

[9] The occurrence of SSW is inferred from the positive zonal mean temperature difference between the latitudes 90°N and 60°N shown in Figure 2a. As can be seen from

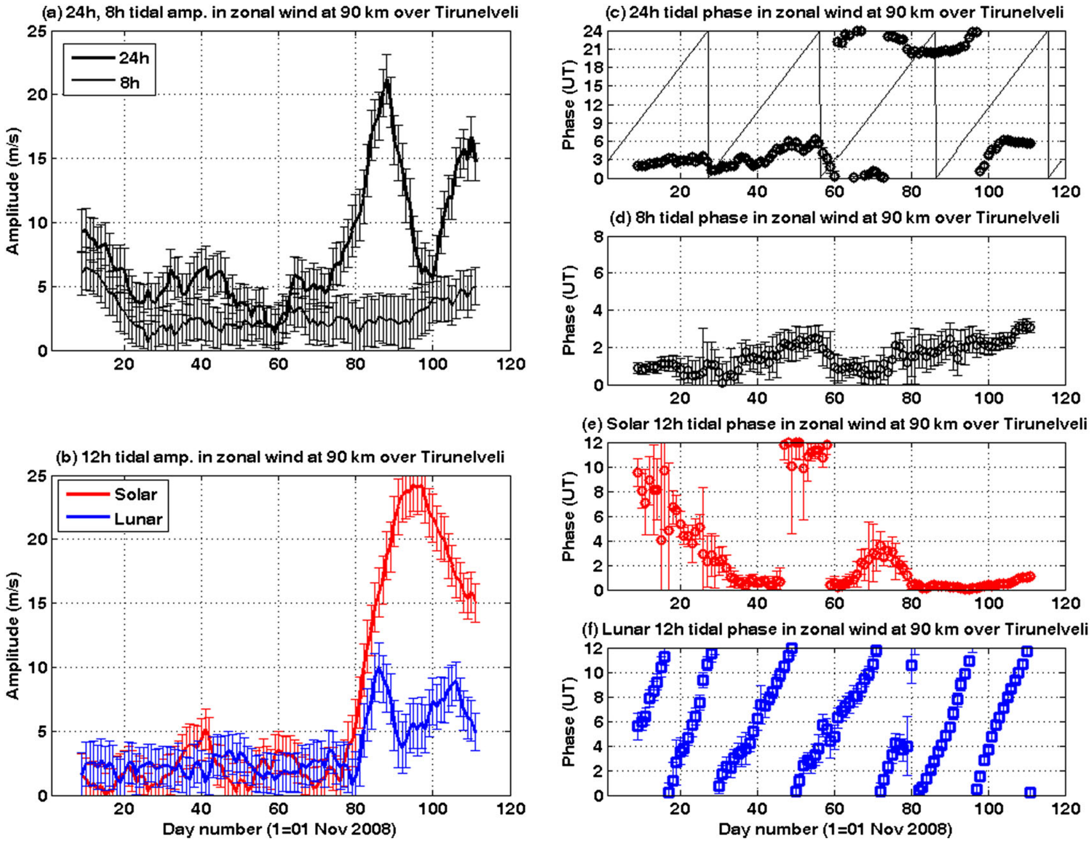

Figure 3. (a) Diurnal and terdiurnal tidal amplitude, (b) solar and lunar semidiurnal tidal amplitude, (c) diurnal tidal phase, (d) terdiurnal phase, (e) solar semidiurnal tidal phase, and (f) lunar semidiurnal phase in zonal wind at 90 km over Tirunelveli. The lunar age is plotted in Figure 3c for reference ($\nu = 0$ refers to new moon day) for the time interval of 1–120 d starting from 1 November 2008. The errors in the computation of tidal amplitudes and phases are also shown.

the figure, there is a sudden increase in the temperature difference from –13 K on day number 81 to 26 K on day number 82. The positive temperature difference persists during day numbers 82–87 (21–26 January 2009) and again during day numbers 102–107. Large deceleration of zonal mean zonal wind occurs in association with the SSW and it begins from day number 70 from 68 m/s to –34 m/s on day number 89 (Figure 2a). As this SSW is associated with the reversal of winds from eastward to westward, this event is a major SSW. It is an unprecedented event, as described by *Manney et al*. [2009] with the westward winds persisted for a long time during the day numbers 85–114. The EEJ strength over Tirunelveli shows negative depression indicating counter electrojet events during day numbers 83–90 (Figures 2b and 2c). During this period, the *Ap* value is less than 12 (Figure 2d) indicating that it is a geomagnetically quiet period. Large CEJ occurs on day numbers 88 and 89 with the maximum depression of about 53 nT, with a delay of only a few days after the large polar stratospheric temperature difference (Figure 2a). Besides, a few CEJ events occur around the day number 100 also. However, the events are preceded by geomagnetically disturbed day (day number 96) as the *Ap* value is greater than 12 (Figure 2d).

[10] As EEJ current system is driven by tidal winds, the daily variation of tidal amplitudes and phases over Tirunelveli are shown in Figure 3. The solar diurnal tide gets significantly enhanced from 5 m/s on day number 73 to 21 m/s on day number 88 followed by a sudden decrease to 7 m/s on day number 100 and increase to 17 m/s on day number 110. The solar semidiurnal tide also shows large enhancement from 1 m/s on day number 76 to 24 m/s on day number 96. Note that the solar semidiurnal tidal amplitude is less than 5 m/s before the onset of the SSW event. The terdiurnal tidal amplitude does not show any significant enhancement. The lunar tidal amplitudes are slightly larger than solar semidiurnal tidal amplitudes before the onset of the SSW. After the onset, lunar tidal amplitudes are larger than their pre-SSW onset values, but they are less than solar tidal amplitudes. A ~20 d oscillation can be observed in lunar tidal amplitudes during 61–120 with larger amplitudes on day numbers 86 and 106 with amplitudes 10 and 9, respectively, and smaller amplitude (4 m/s) on day number 92. Note that 1400–1700 h averaged EEJ closely resembles the variation of lunar tidal amplitudes than solar tidal amplitudes. Also note that there are moderately disturbed days during this period.

[11] The diurnal tidal phase in zonal wind shows distinct character during the SSW event. The phase shifts to local midnight during the SSW event from morning hours before and after the SSW event. The solar semidiurnal tidal phase remains at 0000–0100 UT during the SSW event and it shifts

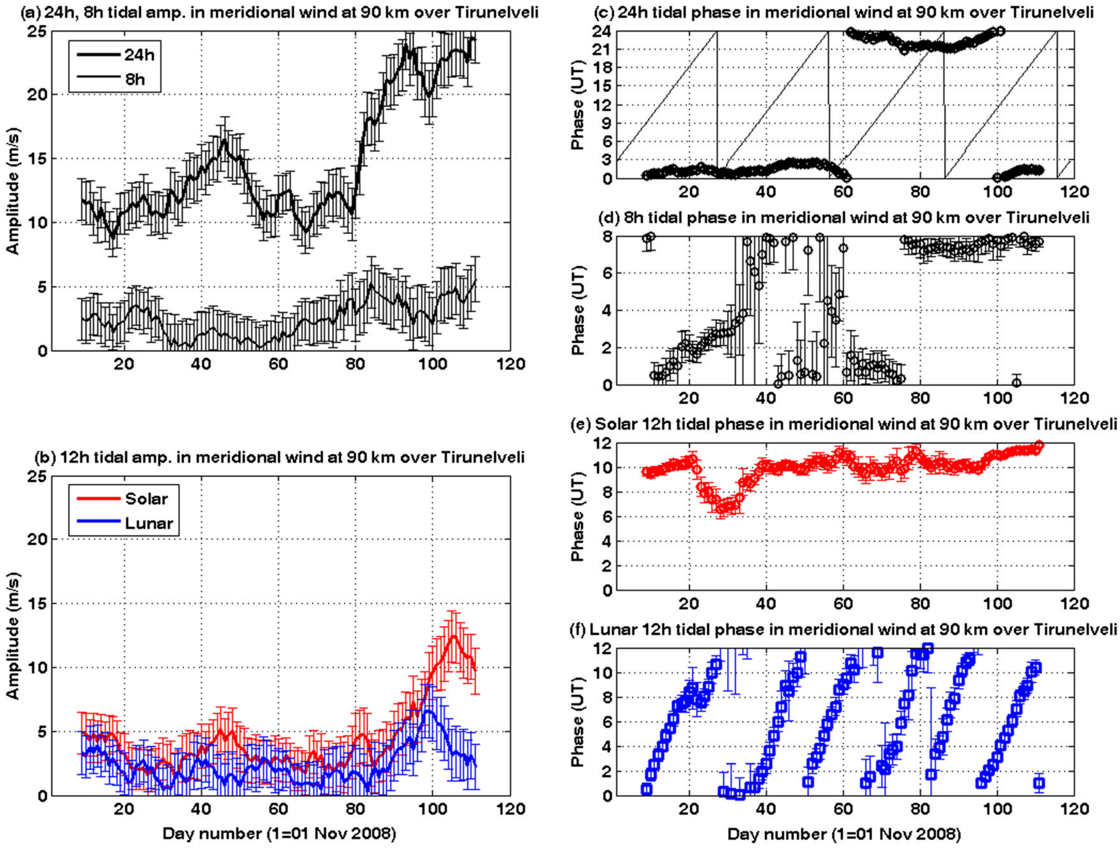

Figure 4. Same as Figure 3, but in meridional wind at 90 km over Tirunelveli.

to 0200–0300 UT for a few days just before onset of the SSW event. The lunar tidal phase shows progressive shift to later hours. The lunar semidiurnal tidal phase does not show any variation with altitude on day numbers 86 and 106, when the amplitude of lunar tide is larger (not shown). *Paulino et al*. [2012] also observed constant phase variation with altitude for lunar tides.

[12] The diurnal tidal amplitude in meridional winds also shows enhancement after the day number 80 and it remains with larger amplitudes of 20–25 m/s after the day numbers 89 until the end of observation period shown in Figure 4. Although the amplitude of solar and lunar tidal amplitudes in meridional winds is smaller than those in zonal winds, they also show larger amplitudes after the day number 80. The peak amplitudes of solar semi and lunar tidal amplitudes are about 12 m/s and 7 m/s on days 105 and 99, respectively. The diurnal tidal phase shifts slightly to earlier morning local time hours (2000–2400 UT) during day numbers 60 and 100. Both lunar and solar semidiurnal tidal phases do not show any marked change in association with the SSW.

[13] As can be observed in Figure 5, the amplitude of solar semidiurnal tide in EEJ strength over Tirunelveli is less than that of diurnal tide before the onset of SSW events, although both are increasing a few days before the onset. However, during the SSW, the semidiurnal tidal amplitude becomes comparable and even larger than diurnal tidal amplitude. Unlike in zonal and meridional winds at 90 km, the amplitude of terdiurnal tide in EEJ strength is comparable to that of diurnal tide. It is consistent with the World Atmosphere Model simulations by *Fuller-Rowell et al*. [2010, 2011], who suggested that an increase in the terdiurnal tidal amplitude in the lower thermosphere would change the local time variation of the electrodynamic response with the dayside vertical drift to be larger and occur earlier and for the afternoon minimum to be smaller. As the terdiurnal tide is not observed prominently in local mesospheric winds but observed in EEJ, it appears that it could be due to the influence of midlatitude tidal winds with strong terdiurnal component. The lunar semidiurnal tidal amplitudes in EEJ strength are nearly two times less than that of their solar counterpart during the SSW event, although both the solar and the lunar tidal amplitudes show large values after the day number 80. *Yamazaki et al*. [2012] suggested that variability of the geomagnetic lunar tide during the northern winter is closely linked with dynamical changes in the lower stratospheric parameters associated with SSWs. The diurnal tidal phase in EEJ strength prevails around 6–9 UT and it shifts to early hours (3–6 UT). The terdiurnal tidal phase advances to early hours, as day progresses. Both diurnal and solar semidiurnal tidal phases are around 5 UT. The lunar semidiurnal tidal phases shift to later hours.

[14] *Fejer et al*. [2010] observed large semidiurnal perturbations in electrojet intensity close to new and full moons and the perturbation shifts to later local times with the lunar age indicating the enhancement of lunar tidal effects during the SSW events. In the present study, the minimum EEJ strength over

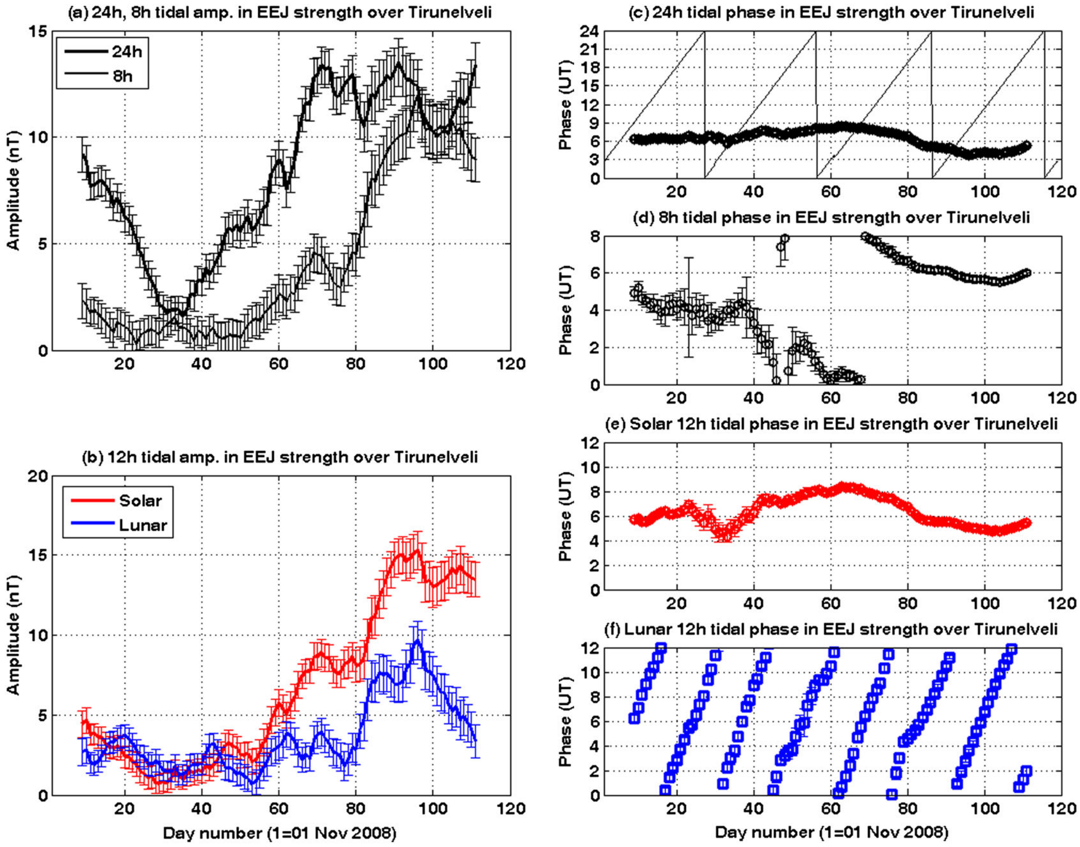

Figure 5. Same as Figure 3, but in equatorial electrojet strength over Tirunelveli.

Tirunelveli on a given day and the corresponding time is shown in Figure 6 for the day numbers 61–101. The minimum EEJ indicates that the largest depression in the horizontal component of geomagnetic field, which indirectly indicates the strength of CEJ and corresponding time denotes the time when the largest depression occurs. From the figure, it is clearly observed that there is no significant phase advancement of the time of the occurrence of minimum EEJ to later hours during the SSW (day numbers 80–90). Although after the SSW event, the time of minimum EEJ strength advances to later hours with 8.5 UT, 9.5 UT, 10.5 UT, and 11.5 UT on day number 101, 102, 104, and 113, respectively, these days are preceded by geomagnetic disturbance. Hence, the lunar tidal influence cannot be solely responsible for the advancement of the phase to later hours. This suggests that lunar tidal influence in EEJ strength appears to be less than solar influence during the SSW event.

4. Discussion and Conclusion

[15] The present study shows enhancement of solar semidiurnal tide in both zonal wind at 90 km and EEJ strength over Tirunelveli. Although there is an enhancement in the lunar tidal amplitude also during SSW 2009, it is much less than that of solar semidiurnal tide. This amplification is not a result of spectral leakage of the solar semidiurnal tide, because its variability is completely different from the lunar tide variability. The diurnal tidal amplitudes in zonal wind and EEJ strength also show large enhancement just before the onset of SSW. However, solar semidiurnal tide dominates diurnal tide during the SSW. There is a distinct behavior in diurnal tidal phase in zonal wind during SSW and it shifts to a few hours earlier. The lunar semidiurnal tide in zonal wind shows advancement in phase to later hours in both zonal wind and EEJ strength.

[16] The main observation of the present study is that the large semidiurnal tide observed during the SSW 2009 is mostly solar driven and partly lunar driven. Many observational and theoretical studies on the lunar signature in mesosphere winds and ionospheric parameters have been reported. Recently, *Fejer et al.* [2010] showed enhanced semidiurnal variations in vertical plasma drifts over Jicamarca associated with an SSW and the time of maximum downward perturbation becomes later on succeeding days and indicated that it could be due to the influence of lunar tide. More recently, *Paulino et al.* [2012] reported enhancement of the mesospheric lunar tide in the Brazilian sector during 2006 SSW. Earlier, *Stening* [1977] suggested that CEJ during SSW may be due to enhanced lunar tide and the SSW might change background conditions, which favor vertical propagation of the lunar tides. The numerical simulations of *Stening et al.* [1997] showed a large change of lunar tides during SSW. There could be a difference in the lunar and solar influences on tides from one warming event to the other. During the 2006 SSW case presented in Figure 7, it may be noted that the minor warming occurred during day numbers 65–67 and 71–80 and a major warming event occurred during day numbers 83–99, which can be inferred

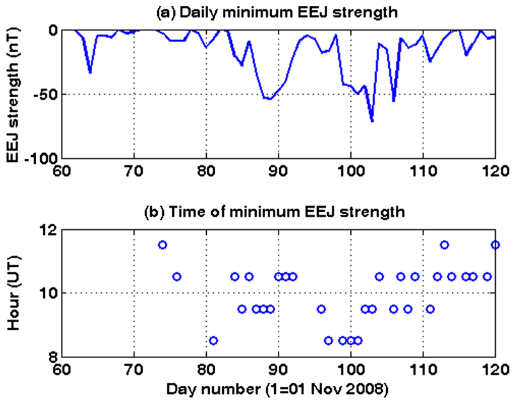

Figure 6. (a) Daily minimum EEJ strength and (b) the corresponding time.

from the positive temperature difference between the latitudes 90°N and 60°N and variations of zonal mean zonal winds at 60°N at 10 hPa (Figure 7a). In this case, the solar tide in zonal wind enhances significantly around day number 80 associated with the major SSW and there is no significant enhancement in lunar tidal amplitude. No significant change is noticed in the solar and lunar tidal variabilities in meridional winds. It may be noted that *Paulino et al*. [2012] observed a large increase in the lunar semidiurnal tide during the SSW in meteor wind observations over Cariri (7.4°S 36.5°W), Cachoeira Paulista (23°S, 45°W), and Santa Maria (29.7°S, 53.7°W). At 96 km, they also reported enhancement of lunar tide at 96 km over Cariri during the first week of December 2005, which is a non-SSW period. However, in the present study, lunar tidal amplitude in EEJ strength is larger than that of solar during day numbers 70–90, as observed by *Paulino et al*. [2012] in the winds over Cariri (7.4°S, 36.5°W). It is not clear how lunar tidal signature in EEJ strength is stronger, when the same is less in the underlying mesospheric tidal winds and is similar in the tidal winds over the Brazilian sector. *Stening* [2011] catalogued the coincidences of SSW events with full/new moons (or not) and the occurrence of CEJ. The table seems to indicate a relationship of SSW occurrence with lunar phase. There seems to be strong correlations of SSW's, lunar phase, and CEJ's but the causal physics connections are not clear. There are also SSW events that are not associated with lunar

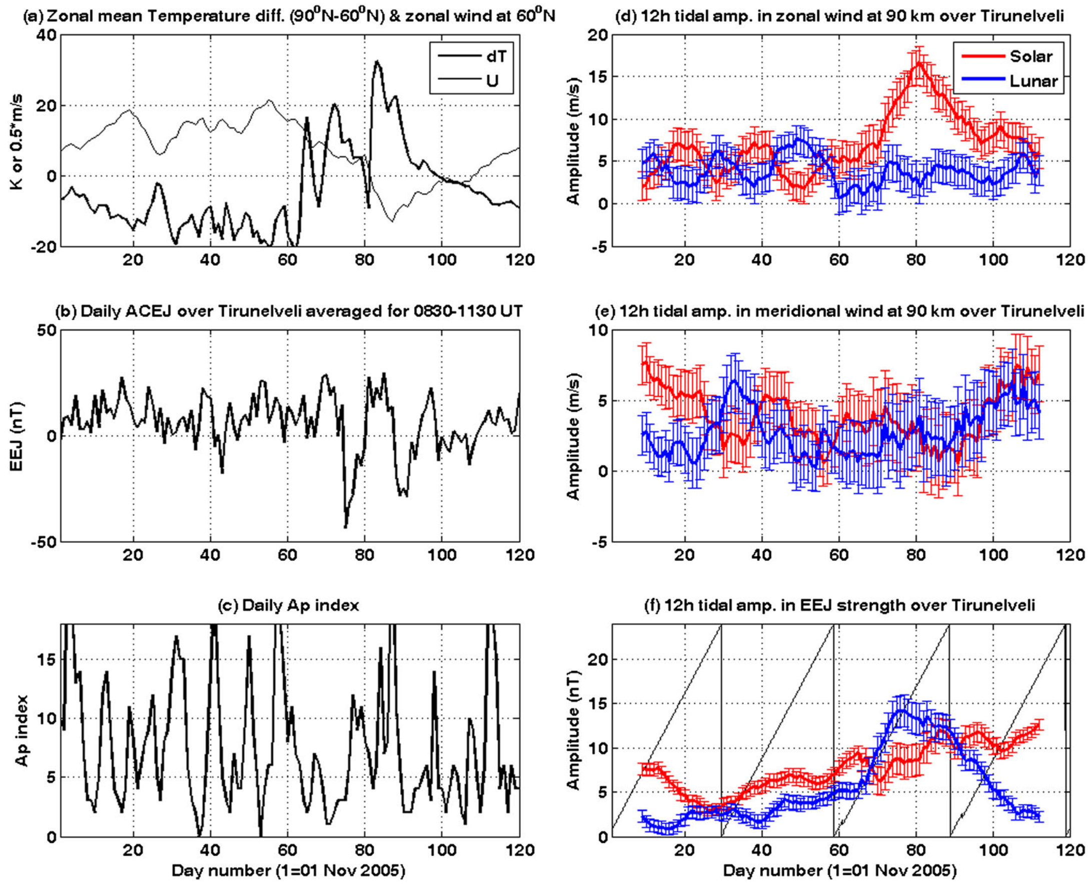

Figure 7. (a) Daily variation of zonal mean temperature difference between the latitudes 90°N and 60°N and zonal mean zonal wind at 60°N; (b) daily afternoon CEJ strength computed by taking average of EEJ strength for 1400–1700 IST (Indian Standard Time, which is 05:30 h ahead of UT; (c) daily *Ap* index; (d) solar and lunar semidiurnal tidal amplitude in zonal wind at 90 km over Tirunelveli; (e) same as Figure 7d, but in meridional wind at 90 km over Tirunelveli; (f) same as Figure 7d, but in EEJ strength over Tirunelveli and the lunar age is also plotted for reference for the time interval of 1–120 d starting from 1 November 2005.

phase. *Stening* [2011] pointed out that the enhancement in the lunar tide during SSW may be coincidental, as the climatological behavior of lunar tide is to enhance during winter. Our observations also show that semidiurnal tide is largely solar driven during the SSW events.

[17] *Park et al*. [2012] noted amplified 13 d modulation in EEJ strength during SSW and the absence of this modulation during non-SSW years and attributed this due to the effect of lunar tides. It may be noted that 16 d wave is quite dominant during the SSW events [*Vineeth et al*., 2010; *Sripathi and Bhattacharyya*, 2012]. As the period of quasi 16 d wave may vary between 12 and 20 d, the 13 d modulation may also be due to modulation by quasi 16 d wave. Recently, *Pedatella et al*. [2012] showed from their simulations using the Whole Atmosphere Community Model that the lunar tidal influences are larger only above 120 km. The enhancement of semidiurnal tide may also be due to planetary wave tidal interaction [*Pedatella and Forbes*, 2010] or accumulation of ozone at low-latitudes and hence variations in the ozone heating [*Sridharan et al*., 2012; *Goncharenko et al*., 2012] or zonal mean zonal winds or combination of all these [*Pedatella et al*., 2012].

[18] Although the present study indicates that the low-latitude mesospheric semidiurnal tide over Tirunelveli during SSW 2009 is largely solar and it is consistently observed during the SSW 2006 also, the large lunar semidiurnal tide observed in the EEJ strength during the SSW 2006 without having large lunar semidiurnal tide in the underlying mesospheric winds is puzzling. More observational and theoretical works are necessary to understand the relative importance of solar and lunar tides on the occurrence of CEJ and its relationship with SSW.

[19] **Acknowledgments.** The authors acknowledge the European Center for Medium Range Weather Forecasting for ERA-Interim data sets used in this study. They thank the technical staff of Indian Institute of Geomagnetism, who maintain and successfully run the geomagnetic observatories at Tirunelveli and Alibag and the MF radar at Tirunelveli.

References

Anderson, D., and E. A. Araujo-Pradere (2010), Sudden stratospheric warming event signatures in daytime E _ B drift velocities in the Peruvian and Philippine longitude sectors for January 2003 and 2004, *J. Geophys. Res.*, *115*, A00G05, doi:10.1029/2010JA015337.

Berrisford, P., D. Dee, K. Fielding, M. Fuentes, P. Kallberg, S. Kobayashi, and S. Uppala (2009), The ERA-Interim Archive. European Centre for Medium Range Weather Forecasts, Shinfield Park, Reading, Berkshire RG2 9AX, United Kingdom, 1–16.

Chapman, S., and R. S. Lindzen (1970), *Atmospheric Tides*, Gordon and Breach, New York.

Chau, J. L., B. G. Fejer, and L. P. Goncharenko (2009), Quiet variability of equatorial E × B drifts during a sudden stratospheric warming event, *Geophys. Res. Lett.*, *36*, L05101, doi:10.1029/2008GL036785.

Eccles, V., D. D. Rice, J. J. Sojka, C. E. Valladares, T. Bullett, and J. G. Chau (2011), Lunar atmospheric tidal effects in the plasma drifts observed by the Low-Latitude Ionospheric Sensor Network, *J. Geophys. Res.*, *116*, A07309, doi:10.1029/2010JA016282.

Fejer, B. G., M. E. Olson, J. L. Chau, C. Stolle, H. Lühr, L. P. Goncharenko, K. Yumoto, and T. Nagatsuma (2010), Lunar-dependent equatorial ionospheric electrodynamic effects during sudden stratospheric warmings, *J. Geophys. Res.*, *115*, A00G03, doi:10.1029/2010JA015273.

Forbes, J. M., and X. Zhang (2012), Lunar tide amplification during the January, 2009 stratospheric warming event: Observations and theory, *J. Geophys. Res.*, doi:10.1029/2012JA017963.

Fuller-Rowell, T., F. Wu, R. Akmaev, T.-W. Fang, and E. Araujo-Pradere (2010), A whole atmosphere model simulation of the impact of a sudden stratospheric warming on thermosphere dynamics and electrodynamics, *J. Geophys. Res.*, *115*, A00G08, doi:10.1029/2010JA015524.

Fuller-Rowell, T., H. Wang, R. Akmaev, F. Wu, T.-W. Fang, M. Iredell, and A. Richmond (2011), Forecasting the dynamic and electrodynamic response to the January 2009 sudden stratospheric warming, *Geophys. Res. Lett.*, *38*, L13102, doi:10.1029/2011GL047732.

Goncharenko, L. P., A. J. Coster, J. L. Chau, and C. E. Valladares (2010a), Impact of sudden stratospheric warmings on equatorial ionization anomaly, *J. Geophys. Res.*, *115*, A00G07, doi:10.1029/2010JA015400.

Goncharenko, L. P., A. J. Coster, R. A. Plumb, and D. I. V. Domeisen (2012), The potential role of stratospheric ozone in the stratosphere-ionosphere coupling during stratospheric warmings, *Geophys. Res. Lett.*, *39*, L08101, doi:10.1029/2012GL051261.

Goncharenko, L. P., J. L. Chau, H.-L. Liu, and A. J. Coster (2010b), Unexpected connections between the stratosphere and ionosphere, *Geophys. Res. Lett.*, *37*, L10101, doi:10.1029/2010GL043125.

Hanuise, C., C. Mazaudier, P. Vila, M. Blanc, and M. Crochet (1983), Global dynamo simulation of ionospheric currents and their connection with the equatorial electrojet and counter electrojet: A case study, *J. Geophys. Res.*, *88*(A1), 253–270, doi:10.1029/JA088iA01p00253.

Kane, R. P. (1973), Comparison of geomagnetic changes in India and the POGO data, *J. Atmos. Terr. Phys.*, *35*, 1249–1252.

Manney, G. L., K. Kruger, J. L. Sabutis, S. A. Sena, and S. Pawson (2005), The remarkable 2003-04 winter and other recent warm winters in the Arctic stratosphere since the late 1990s, *J. Geophys. Res.*, *110*, D04107, doi:10.1029/2004JD005367.

Manney, G. L., M. J. Schwartz, K. Krüger, M. L. Santee, S. Pawson, J. N. Lee, W. H. Daffer, R. A. Fuller, and N. J. Livesey (2009), Aura Microwave Limb Sounder observations of dynamics and transport during the record-breaking 2009 Arctic stratospheric major warming, *Geophys. Res. Lett.*, *36*, L12815, doi:10.1029/2009GL038586.

Matsuno, T. (1971), A dynamical model of the stratospheric sudden warming, *J. Atmos. Sci.*, doi:10.1175/1520-0469.

Park, J., H. Lühr, M. Kunze, B. G. Fejer, and K. W. Min (2012), Effect of sudden stratospheric warming on lunar tidal modulation of the equatorial electrojet, *J. Geophys. Res.*, *117*, A03306, doi:10.1029/2011JA017351.

Paulino, A. R., P. P. Batista, B.R. Clemeshaa, R.A. Buriti, and N. Schuch (2012), An enhancement of the lunar tide in the MLT region observed in the Brazilian sector during 2006 SSW, *J. Atmos. Sol.-Terr. Phys.*, doi: 10.1016/j.jastp.2011.12.015.

Pedatella, N. M., and J. M. Forbes (2010), Evidence for stratosphere sudden warming-ionosphere coupling due to vertically propagating tides, *Geophys. Res. Lett.*, *37*, L11104, doi:10.1029/2010GL043560.

Pedatella, N. M., H.-L. Liu, A. D. Richmond, A. Maute, and T.-W. Fang (2012), Simulations of solar and lunar tidal variability in the mesosphere and lower thermosphere during sudden stratosphere warmings and their influence on the low-latitude ionosphere, *J. Geophys. Res.*, doi:10.1029/2012JA017858.

Sandford, D. J., H. G. Muller, and N. J. Mitchell (2006), Observations of lunar tides in the mesosphere and lower thermosphere at Arctic and middle latitudes, *Atmos. Chem. Phys.*, *6*, 4117–4127.

Sridharan, S., and S. Sathishkumar (2008), Seasonal and interannual variations of gravity wave activity in the low-latitude mesosphere and lower thermosphere over Tirunelveli (8.7_ N, 77.8_ E), *Ann. Geophys.*, *26*, 3215–3223.

Sridharan, S., S. Sathishkumar, and S. Gurubaran (2009), Variabilities of mesospheric tides and equatorial electrojet strength during major stratospheric warming events, *Ann. Geophys.*, *27*, 4125–4130, doi:10.5194/angeo-27-4125-2009.

Sridharan, S., S. Sathishkumar, and S. Gurubaran (2012), Variabilities of mesospheric tides during sudden stratospheric warming events of 2006 and 2009 and their relationship with ozone and water vapour, *J. Atmos. Sol. Terr. Phys.*, *78–79*, 108–115.

Sripathi, S., and A. Bhattacharyya (2012), Quiet time variability of the GPS TEC and EEJ strength over Indian region associated with major sudden stratospheric warming events during 2005/2006, *J. Geophys. Res.*, *117*, A05305, doi:10.1029/2011JA017103

Stening, R. J. (1977), Electron density changes associated with the equatorial electrojet, *J. Atmos. Terr. Phys.*, *39*, 157–164, doi:10.1016/0021-9169(77)90109-X.

Stening, R. J., J. M. Forbes, M. E. Hagan, and A. D. Richmond (1997), Experiments with a lunar atmospheric model, *J. Geophys. Res.*, *102*, 13,465–13,471, doi.10.1029/97JD00778.

Stening, R. J. (2011), Lunar tide in the equatorial electrojet in relation to stratospheric warmings, *J. Geophys. Res.*, *116*, A12315, doi:10.1029/2011JA017047.

Stening, R. J. (1991), Variability of the equatorial electrojet: Its relations to the Sq current system and semidiurnal tides, *Geophys. Res. Lett.*, *18*(11), 1979–1982, doi:10.1029/91GL02413.

Stening, R. J., A. H. Manson, C. E. Meek, and R. A. Vincent (1994), Lunar tidal winds at Adelaide and Saskatoon at 80 to 100 km heights, 1985–1990, *J. Geophys. Res.*, *99*, 13,273–13,280.

Stening, R. J., C. E. Meek, and A. H. Manson (1996), Upper atmosphere wind systems during reverse equatorial electrojet events, *Geophys. Res. Lett.*, *23*, 3243–3246, doi:10.1029/96GL02611.
Vineeth, C., T. K. Pant, K. K. Kumar, and S. G. Sumod (2010), Tropical connection to the polar stratospheric sudden warming through quasi 16-day planetary wave, *Ann. Geophys.*, *28*, 2007–2013.
Yamazaki, Y., A. D. Richmond, and K. Yumoto (2012), Stratospheric warmings and the geomagnetic lunar tide: 1958–2007, *J. Geophys. Res.*, *117*, A04301, doi:10.1029/2012JA017514.